Sex and Mitonuclear Adaptation in Experimental *Caenorhabditis elegans* Populations

Riana I. Wernick,*[,1] Stephen F. Christy,[†,1] Dana K. Howe,* Jennifer A. Sullins,[†] Joseph F. Ramirez,[†] Maura Sare,[‡] McKenna J. Penley,[‡] Levi T. Morran,[‡] Dee R. Denver,* and Suzanne Estes[†,2]

*Department of Integrative Biology, Oregon State University, Corvallis, Oregon 97331, [†]Department of Biology, Portland State University, Oregon 97201, and [‡]Department of Biology, Emory University, Atlanta, Georgia 30322

ABSTRACT To reveal phenotypic and functional genomic patterns of mitonuclear adaptation, a laboratory adaptation study with *Caenorhabditis elegans* nematodes was conducted in which independently evolving lines were initiated from a low-fitness mitochondrial electron transport chain (ETC) mutant, *gas-1*. Following 60 generations of evolution in large population sizes with competition for food resources, two distinct classes of lines representing different degrees of adaptive response emerged: a low-fitness class that exhibited minimal or no improvement compared to the *gas-1* mutant ancestor, and a high-fitness class containing lines that exhibited partial recovery of wild-type fitness. Many lines that achieved higher reproductive and competitive fitness levels were also noted to evolve high frequencies of males during the experiment, consistent with adaptation in these lines having been facilitated by outcrossing. Whole-genome sequencing and analysis revealed an enrichment of mutations in loci that occur in a *gas-1*-centric region of the *C. elegans* interactome and could be classified into a small number of functional genomic categories. A highly nonrandom pattern of mitochondrial DNA mutation was observed within high-fitness *gas-1* lines, with parallel fixations of nonsynonymous base substitutions within genes encoding NADH dehydrogenase subunits I and VI. These mitochondrial gene products reside within ETC complex I alongside the nuclear-encoded GAS-1 protein, suggesting that rapid adaptation of select *gas-1* recovery lines was driven by fixation of compensatory mitochondrial mutations.

KEYWORDS compensatory mutation; cytonuclear coevolution; epistasis; heteroplasmy; outcrossing; parallel evolution

OWING to the evolutionary history of the nuclear DNA (nDNA) and mitochondrial DNA (mtDNA) genomes, the most critical function of mitochondria—production of ATP via oxidative phosphorylation—relies upon the interaction of nDNA- and mtDNA-encoded protein subunits that form the mitochondrial electron transport chain (ETC). Because most ETC components are subject to this dual genetic control, maintenance of favorable mitonuclear epistatic interactions is key to proper mitochondrial functioning (Rand *et al.* 2004; Harrison and Burton 2006; Dowling *et al.* 2007, 2008; Azevedo *et al.* 2009; Arnqvist *et al.* 2010; Montooth *et al.* 2010; Lane 2011). Evidence of tight coevolution between the nDNA- and mtDNA-encoded subunits is provided by cases of "mitonuclear mismatch," wherein hybrid lineages experience ETC deficiencies and reduced fitness (Shoubridge 2001; Rawson and Burton 2002; Sackton *et al.* 2003). How this genomic coevolution is maintained given the radically different population biologies, and baseline mutational rates and processes (Denver *et al.* 2000), experienced by nDNA and mtDNA is not well understood. In particular, many features of mitochondrial biology would appear to promote high rates of deleterious mutation accumulation compared to the nuclear genome, including: maternal inheritance and no or infrequent recombination leading to reduced effective population size (N_e) (Ballard and Whitlock 2004), and limited DNA repair [reviewed in Alexeyev *et al.* (2013)]. Support comes from comparative sequence analyses revealing high nucleotide substitution rates in mtDNA (Lynch 1996) and phylogenetic analyses suggesting that adaptive evolution in nDNA-encoded ETC genes has been accelerated to compensate for degradation of their mtDNA counterparts (Osada and Akashi 2012; Barreto and Burton 2013; Havird *et al.* 2015b).

doi: https://doi.org/10.1534/genetics.119.301935
Manuscript received August 14, 2018; accepted for publication January 17, 2019; published Early Online January 21, 2019.
Supplemental material available at Figshare: https://doi.org/10.25386/genetics.7609925.
[1]These authors contributed equally to this work.
[2]Corresponding author: Department of Biology, Room 246, Science, Research, and Teaching Center, Portland State University, 1719 SW 10 Ave., Portland, OR 97201. E-mail: estess@pdx.edu

Such findings have helped to instill the notion that selection on mtDNA is too weak to avoid deleterious mutation accumulation, and have led to the formation of the nuclear compensation hypothesis (Burton *et al.* 2013; Havird and Sloan 2016), which posits that mitonuclear matching is maintained to a large extent by the nDNA genome.

The above studies support a model of mitonuclear coevolution in which all of the compensatory or adaptive changes occur in the nuclear genome; however, a recent analysis found no difference in the efficacy of purifying selection between mtDNA and nDNA genomes of flies and humans (Cooper *et al.* 2015). These results add to evidence for efficient purifying selection in mtDNA, particularly on genes encoding core ETC subunits (Bazin *et al.* 2006; Ellison and Burton 2006; Meiklejohn *et al.* 2007; Burton *et al.* 2013; Cooper *et al.* 2015). Theory also shows that the effect of uniparental inheritance [*i.e.*, maintenance of high among-lineage variance in mutation load (Bergstrom and Pritchard 1998)] can prevent or retard mtDNA decay under most circumstances (Hadjivasiliou *et al.* 2013; Radzvilavicius *et al.* 2017). Finally, many features of mitochondria may favor genome integrity and efficient selection (Rand 2008), including life cycles involving fission, fusion, and autophagy that may purge damaged mtDNA genomes (Twig *et al.* 2008; Kuznetsov and Margreiter 2009; Kowald and Kirkwood 2011); multiple levels of selection (Rand 2001; Taylor *et al.* 2002); and mechanisms promoting oocyte-specific mtDNA stability (de Paula *et al.* 2013).

The mitochondrial ETC is an excellent system for addressing the roles and patterns of adaptive mutations responsible for maintaining mitonuclear integration. Here, we report the first direct, nonretrospective study of adaptive evolution of the mitochondrial ETC, applying an experimental genomics approach with a well-studied ETC-deficient strain of *Caenorhabditis elegans* nematodes, *gas-1*. The study builds upon our previous work describing mitochondrial heteroplasmy (Wernick *et al.* 2016), and patterns and phenotypic consequences of nuclear mutations (Christy *et al.* 2017) accumulating under drift within the same strain. The goal of the present study was to understand the capacity of new mutations to restore ancestral levels of fitness and phenotypes within replicate lineages of *gas-1* nematodes experimentally evolved under conditions of efficient selection; *i.e.*, large N_e. With large N_e, selection is generally more efficient at both purging deleterious mutations and fixing beneficial mutations. Still, only a small fraction of newly arising beneficial mutations will achieve fixation within populations; the asymptotic probability is equivalent to twice the selection coefficient when population size is large. Similarly, large populations are not immune to deleterious mutation accumulation, especially if mutation rates are high and individual mutational effects are small. Mutations with effects $<<1/(2N_e)$ are expected to be governed exclusively by random genetic drift, causing them to accumulate at close to the neutral rate [see chapter 3 in Kimura (1983)]. However, previous results from our group and others are consistent with the selective effects of the majority of novel deleterious and beneficial mutations being sufficiently large for their frequencies to be efficiently shaped by selection (Estes *et al.* 2004; Denver *et al.* 2010; Phillips *et al.* 2015; Konrad *et al.* 2017). How these competing evolutionary forces operate on nuclear and mitochondrial mutations to yield an adaptive mitonuclear response is an ideal question for the application of an experimental evolution approach.

Here, we report results of a "recovery experiment" [compare with Estes and Lynch (2003)] wherein replicate lines of a *gas-1* ETC mutant ancestor were maintained in large population sizes (1000-individual bottlenecks), with efficient natural selection prior to phenotyping and whole-genome sequence analysis for mutation detection. Surprisingly, between generations 20 and 30 of the experiment, we noted that several *gas1* recovery (RC) line populations contained appreciable frequencies (up to what appeared to be ~50%) of males, a pattern that persisted throughout the experiment. *C. elegans* is an androdiecious species, with populations normally comprising self-fertilizing hermaphrodites (XX) and extremely rare males (hemizygous, X0) with whom hermaphrodites can outcross. Outcrossed offspring exhibit 50:50 sex ratios, but males are rapidly lost from populations under most circumstances (Anderson *et al.* 2010). This observation presented the opportunity to compare evolution under selfing *vs.* outcrossing.

Materials and Methods

Strains

Twenty-four RC lines were generated from a *C. elegans gas-1* mutant previously utilized for an mutation-accumulation (MA) study (Wernick *et al.* 2016; Christy *et al.* 2017). The *C. elegans gas-1* gene is nuclear-encoded and orthologous to human *NDUFS2* (83% protein similarity); it encodes a core subunit of ETC complex I, which helps to form the quinone-binding pocket (Vasta *et al.* 2011; Shiraishi *et al.* 2012). The *gas-1(fc21)* allele is a single-base pair missense mutation (Kayser *et al.* 1999) associated with deleterious phenotypes including reduced fecundity, reduced complex I-dependent metabolism (Kayser *et al.* 2004), hypersensitivity to oxidative stress owing to increased reactive oxygen species (ROS) production (Kayser *et al.* 2001, 2004), and low ATP levels relative to wild-type (Lenaz *et al.* 2006). The original *gas-1* mutant, derived from ethyl methanesulfonate (EMS) mutagenesis (Kayser *et al.* 1999), was obtained from the *Caenorhabditis* Genetics Center (University of Minnesota) and backcrossed to Bristol N2 for 10 generations in an attempt to create an isogenic mutant strain. Both strains are expected to be homozygous at all loci. The resulting *gas-1* strain, referred to hereafter as *gas-1* G0, was allowed to recover from freezing for two generations at 20° on Nematode Growth Medium-Lite (NGML) plates seeded with *Escherichia coli* OP50-1. RC lines were initiated with 24 randomly chosen L4-stage offspring from a single *gas-1* G0 parent; the lines

were then passaged in large population sizes ($N = 1000$) for 60 generations, a timescale sufficient for fitness recovery in other mutant strains (Estes *et al.* 2011). Transfer population sizes were estimated via sample egg counts and nonoverlapping generations were maintained by standard age synchronization of cultures prior to each transfer. Samples of each RC line were frozen at five-generation intervals.

Prior to all phenotypic experiments, strains were allowed to recover from freezing for two-to-three generations at 20° on NGML plates containing 20 μg/ml streptomycin and *E. coli* OP50-1. For the ROS and nondisjunction assays, lines were age-synchronized by standard bleach treatment prior to each assay.

Conventional fitness assay

Daily offspring production and life span were assayed for N2, *gas-1* G0, and the generation-60 *gas-1* RC lines following established methods (Estes and Lynch 2003). One adult hermaphrodite from each of five replicates was transferred to an individual plate to lay eggs for 5 hr, creating an age-synchronous cohort. One offspring from each parent was then transferred to an individual plate, resulting in a total of five individuals from each *gas-1* RC line, and 9–10 individuals each of N2 and *gas-1* G0 control(s) or lines assayed. The number of unhatched and presumably inviable eggs were also counted. Life span was calculated as days lived from the egg stage; survival rates were calculated from the same data set. Eight worms died due to desiccation after crawling up the side of Petri plates and were omitted from analysis. Data were used to calculate mean absolute (total reproductive output, W) and relative fitness (ω) of the *gas-1* G0 mutant compared to N2, and of each *gas-1* RC line compared to the *gas-1* G0 ancestor. Relative fitness of each individual was computed as: $\omega = \Sigma e^{-rx} l(x) m(x)$, where $l(x)$ is the number of worms surviving to day x, $m(x)$ is the fecundity at day x, and r is the mean intrinsic population growth rate of the assay-specific N2 or *gas-1* control as appropriate. The latter was calculated by solving Euler's equation for r from the equation $\omega = \Sigma e^{-rx} l(x) m(x) = 1$ using an average value of $l(x)m(x)$ for the controls. We set $x = 4.75$ on the first reproductive day [compare with Vassilieva *et al.* (2000)].

Competitive fitness assay

We also performed competitive fitness assays following the methods of Morran *et al.* (2009) on a subset of 14 RC lines chosen to represent two fitness classes revealed by the above conventional assays. These assays more closely simulate the environment in which the worms were experimentally evolved, thereby allowing us to avoid potential genotype-by-environment interactions. Assays were conducted in two blocks to obtain a total of two-to-eight replicates of RC lines (with a goal of five) and five replicates of *gas-1* G0. Competitions began by mixing roughly equal numbers of age-synchronized L4 RC individuals with L4 GFP-marked tester strain (JK2735) individuals on *E. coli*-seeded plates. The goal was to plate 500 individuals of each strain; however, actual experimental numbers ranged from 402 to 666 individuals. The two strains were allowed to compete (and to mate if experimental males were present) and the resulting L4 offspring were counted after three generations. The assay followed the same passaging protocol used in recovery, including age synchronization, as described above. GFP- = expression is dominant in the tester strain, meaning that fitness would be underestimated for the experimental lines, or the *gas-1* G0 or N2 control strain, if outcrossing occurred. Care was therefore taken to ensure that no tester males were included in the competition assays. After three generations of passage, the ratio of non-GFP-marked experimental or control offspring to GFP-marked offspring was calculated for each replicate. These ratios were used to gauge competitive fitness of the RC lines, and the N2 and *gas-1* G0 strains, relative to each other.

Life history data analysis

Differences between *gas-1* G0 and N2 life history trait means and variances were previously reported from a separate data set (Christy *et al.* 2017); we also calculated mean trait differences between the two strains from the current data set using two-way Student's t-tests. Trait differences between *gas-1* RC lines and *gas-1* G0 were evaluated with two-way mixed-model ANOVAs: $y = strain + line(strain) + \varepsilon$, with *strain*—*gas-1* G0 or *gas-1* RC as a fixed effect, and *line*(*strain*) (each RC line nested within *gas-1* RC) as a random effect using the expected mean squares method as applied in JMP12 (SAS). We compared the mean trait values for each RC line with the ancestral *gas-1* G0 using Dunnett's method. For the RC lines, within- and among-line components of variance were calculated using restricted maximum likelihood as applied in JMP12 (SAS), while restricting variance estimates to be positive. We tested the model: $y = \mu + RC\,line + \varepsilon$, wherein *RC line* is a random effect and represents among-line variance and ε represents the within-line component of variance. A frequency distribution of *gas-1* RC line fitness relative to *gas-1* G0 was created using least squares means for the *gas-1* RC lines derived from the line(strain) term above. We calculated Spearman's rank correlation coefficients to evaluate the relationship between line-specific mean relative and competitive fitness measures.

Male frequency, outcrossing, and nondisjunction assays

Because increased frequencies of males were noted in several RC lines around generation 20–30 of the 60-generation experiment, we assayed male frequency for all such *gas-1* RC lines, and on additional *gas-1* RC lines representing a mix of lower- and higher-fitness classes (for a total of 16 RC lines), along with *gas-1* G0 and N2 wild-type worms, following the methods of Denver *et al.* (2010). To test whether RC line males were a result of increased instances of X chromosome nondisjunction leading to the X0 male karyotype, nondisjunction assays were performed on the same lines. Males and hermaphrodites were counted on six replicate plates containing roughly 200 (range: 107–612) age-synchronized young

adult offspring of 10–20 unmated hermaphrodites. Average male to hermaphrodite proportions were then calculated for each *gas-1* RC line, *gas-1* G0, and N2.

To understand whether the evolution of male frequency translated into increased rates of outcrossing or altered mating ability, a small number of crosses were conducted between RC line hermaphrodites and N2 males. Reciprocal crosses (RC line males × N2 hermaphrodites), and crosses between *gas-1* G0 males and RC line hermaphrodites, were attempted, but were largely unsuccessful owing to difficulty in recovering males from previously frozen RC lines and the ancestral mutant. Matings were arranged by pairing single RC line hermaphrodites with single N2 males; the number and sex of the resulting offspring were then assayed. Outcrossing rates were determined by $2(m-\mu)$, where m is the frequency of the male offspring and μ is the rate of X chromosome nondisjunction [modified from equation 3 in Stewart and Phillips (2002)].

We tested a total of 10 RC lines, with five randomly selected from lines that either evolved high male frequency and fitness (RC3, RC9, RC12, RC18, and RC24), or not (RC2, RC8, RC11, RC16, and RC23). For logistical reasons, crosses were not replicated within RC lines. Data were therefore analyzed by grouping RC lines into male and no-male groups. Four replicate N2 male-*gas-1* G0 hermaphrodite crosses were included as a control.

Steady-state ROS levels

In vivo steady-state ROS levels were quantified for a subset of four *gas-1* RC lines, representing a mix of high- and low-fitness classes alongside those of N2 and *gas-1* G0 controls, using our previously established fluorescence microscopy methods (Joyner-Matos *et al.* 2011; Hicks *et al.* 2013; Smith *et al.* 2014) and a Zeiss ([Carl Zeiss], Thornwood, NY) Axio Imager M2 with monochrome Axiocam 506 camera (Advanced Light Microscopy Core, Oregon Health and Science University, Portland, OR). Two imaging blocks were completed with ∼20 worms labeled with MitoSOX Red mitochondrial superoxide indicator (Molecular Probes, Eugene, OR), and five untreated control worms from each RC line and ancestral control strain were imaged at each session.

Illumina HiSeq read mappings and analyses

Whole-genome sequencing was conducted for all 24 RC lines with pooled samples prepared from thousands of first larval (L1)-stage nematodes collected from multiple hermaphrodites; these hermaphrodites were the offspring of a single individual collected from each RC line as previously described (Wernick *et al.* 2016). Restricting genome analyses to L1-stage animals allows us to avoid sampling many mtDNA heteroplasmies that may accumulate in somatic tissues with nematode age. However, the need to sequence pooled samples to have sufficient template DNA prevents us from distinguishing between true heteroplasmy; *i.e.*, multiple mitotypes segregating within an individual, from variation segregating among individuals. Following each Illumina HiSeq run, reads were aligned to the *C. elegans* genome (version WS242) using CLC Genomics Workbench (CLC Bio/QIAGEN, Valencia, CA). All reads were end-paired (2 × 150 bp) and mapped using the following parameters: no masking, mismatch cost = 2, insertion cost = 3, deletion cost = 3, length fraction = 0.98, 75 read fraction = 0.98, global alignment = no, nonspecific match handling = map randomly (Supplemental Material, Table S1). This procedure was previously performed for the *gas-1* G0 progenitor and N2 wild-type control for an in-depth genetic comparison of the two strains (Wernick *et al.* 2016).

Bioinformatic analyses of mtDNA copy number

mtDNA copy number was normalized by nuclear DNA (nDNA) content as described in Wernick *et al.* (2016). Because samples for sequencing were run on the same lane, among-line variation in mtDNA copy number due to variable sequencing coverage should be negligible. Relative mtDNA for each line was calculated as the line-specific average mtDNA coverage divided by the line-specific average coverage of three single-copy nuclear genes: *ama-1*, *ego-1*, and *efl-2*. The AT-rich region of the mitochondrial genome was not considered due to inconsistencies during sequencing created by its repetitive nature.

We tested normalized mtDNA copy number data for normality and variance using Levene's test. We applied a Kruskal–Wallis H test with strain as an explanatory variable to evaluate whether there was a statistically significant increase in mtDNA copy number following evolution in large population sizes. Kruskal multiple comparison *post hoc* tests were applied to evaluate the significance of normalized mtDNA copy number among pairwise comparisons of all lines.

Identification of mtDNA single-base substitutions

Potential line-specific mtDNA variant sites were identified as mitochondrial genome positions differing from the *C. elegans* reference genome (WS242) and not present within our wild-type N2 lab strain. Site-specific variant frequency was calculated by dividing the number of variant calls by the total site coverage. To eliminate false positives resulting from sequencing and PCR artifacts, variants were required to have at least six variant calls, a variant frequency above 2%, and be within two SD of the line-specific per-site mean coverage. We obtained frequency values of the variant nucleotide for all such sites identified in each RC line, *gas-1* G0, and N2. To control for HiSeq3000 error, we conducted subsequent analyses that took into account the probability that the HiSeq3000 erroneously recorded a variant base call.

Identification and characterization of gas-1 RC line nuclear mutations

Candidate SNPs within the nuclear genomes of *gas-1* RC lines were identified as variants from the *C. elegans* reference genome (WS242) and our wild-type N2 lab strain, as previously described in Wernick *et al.* (2016). To eliminate false positives resulting from PCR and sequencing artifacts, the following criteria were applied: (1) at least fivefold coverage, (2) 100% of reads indicated a single nonreference base (*i.e.*, the

mutation was fixed within the population), (3) at least one read present from both the reverse and forward strand, and (4) reads in a given direction varied upon start/end positions. We only considered mutations found in a single line to eliminate false positives associated with cryptic heterozygosity or paralogy following our previous approaches (Denver *et al.* 2009, 2012).

Gene ontology enrichments

Following our previous methods (Christy *et al.* 2017), gene ontology (GO) enrichments were calculated using GoMiner (Zeeberg *et al.* 2003) application build 457 and the GO MySQL Database (MySQL 3.7.13; Oracle Corporation, Cupertino, CA; GO database build 2016-06-07, geneontology.org) for all nuclear DNA SNPs that arose within protein-coding regions of *gas-1* RC lines within three functional domains: biological process, cellular component, and molecular function. We then determined which broader-level functional "GO slim" categories, as defined by the GO Consortium (Version 1.2, 2012-09-21, geneontology.org), were enriched using CateGOrizer (Hu *et al.* 2008). CateGOrizer classifies enriched GO terms into their respective GO slim categories, giving a coarser-scale overview of enrichment patterns. GO slim categories were checked against the GoMiner output to assess statistical significance.

Interactome analysis of gas-1 RC line mutations

Following our previous approaches (Denver *et al.* 2010; Christy *et al.* 2017), GeneOrienteer version 2.25 (Zhong and Sternberg 2006) was used to construct an interactome, the complete list of all genes predicted to interact with the *gas-1* gene, and to determine the extent to which mutated RC line genes showed membership within this network. Specifically, GeneOrienteer calculates log-likelihood ratio scores for pairwise combinations of *C. elegans* genes based on numerous underlying feature data sources (yeast two-hybrid experiments, microarray data, *etc.*) from *C. elegans*, *Drosophila melanogaster*, and *Saccharomyces cerevisiae*. As before in Christy *et al.* (2017), we refer to the comprehensive list of first- and second-degree *gas-1*-interacting genes as the "*gas-1*-centric-interactome." We then identified all genic single-base pair substitution mutations within *gas-1* RC line nuclear and mitochondrial genomes found in genes residing within the *gas-1*-centric interactome.

Data availability

Nematode strains are available upon request. Supplemental figures show the following: Figures S1 and S2: relative and competitive fitness of *gas-1* RC lines, respectively; Figure S3: normalized mtDNA copy number for all *C. elegans* lines; Figure S4: expected and observed percentages of *gas-1* RC line genic mtDNA mutations; Figure S5: chromatograms depicting evolutionary trajectories of two mtDNA variants; Figure S6: GO enrichments and interactome results for *gas-1* RC line mutations; and Figure S7: GO term categorizations for *gas-1* RC line SNPs. Supplemental tables contain the following data: Table S1: Illumina HiSeq run statistics; Table S2: ANOVA results for *C. elegans* life history traits; Table S3: results of mtDNA copy number normalization; Table S4: *gas-1* G0 mutations reverted to wild-type alleles within RC lines; Table S5: mtDNA SNPs; Table S6: nDNA SNPs; and Table S7: *gas-1* RC line SNPs occurring within the *gas-1* interactome. File S1 shows the frequencies within each *gas-1* RC line for all mtDNA positions in which a variant was identified; File S2 shows the frequencies within each *gas-1* MA line for the *fox-1* single-base pair reversion discovered within three *gas-1* RC lines; File S3 contains custom code for simulations reported in Figure S5; and File S4 contains a complete accounting of *gas-1* RC G0 enrichment results. Illumina whole-genome sequence data have been deposited to the Sequence Read Archive database under accession number PRJNA490381. Supplemental material available at Figshare: https://doi.org/10.25386/genetics.7609925.

Results

Evolution of male frequency and bleach resistance during recovery

Approximately midway through the 60-generation evolution experiment, we noted that 6 of the 24 replicate RC lines (RC3, RC8, RC9, RC12, RC18, and RC24) began to generate appreciable numbers of males, atypical of this androdiecious species. Males of each of these lines were observed in active copulation with hermaphrodites, suggesting the occurrence of successful outcrossing. We found no significant rates of X chromosome nondisjunction in any of the *gas-1* RC lines, or *gas-1* G0 and N2 controls. Male frequency assays revealed that only two *gas-1* RC lines, RC9 and RC17, showed statistically significant—although extremely small—increases compared to *gas-1* G0 (Dunnett's test, $\alpha = 0.05$); a major caveat to this finding is that the lines had been frozen prior to assay, and it is notoriously difficult to recover *C. elegans* males after freezing. Thus, although the true frequencies of males being maintained in the *gas-1* RC lines was higher than reflected by these assays, we can be confident that increased male frequency was not due to increased rates of chromosome nondisjunction in select RC lines. Finally, two of the 24 lines, RC20 and RC22 (neither noted to be male generating), became resistant to the bleach treatments required for age synchronization prior to each transfer; these lines required longer bleach treatment to harvest eggs for the next generation. This evolution did not affect the time between transfers or the total number of generations of evolution achieved for these lines.

Evolution of outcrossing

Mating assays found substantial differences in mating abilities among G0 control, no-male, and high-male RC groups ($F_{2,13} = 11.32$, $P = 0.002$). This result was driven by higher outcrossing rates for high-male RC lines compared to no-male RC lines and *gas-1* G0 (Tukey's HSD, $\alpha = 0.05$). Mean

Table 1 Means for life history traits for N2, *gas-1* G0, and *gas-1* RC

	Controls				*gas-1* RC	*gas-1* RC by males			
Character	N2	*gas-1* G0	*t* statistic	*P*-value	All	Yes	No	*t* statistic	*P*-value
Total reproduction	(9) 210.7 ± 18.91	(10) 64.20 ± 11.97	6.688	< 0.0001	(113) 131.0 ± 6.278	(28) 162.9 ± 12.53	(85) 120.5 ± 6.921	3.024	0.0031
Life span	(9) 14.56 ± 2.082	(10) 15.20 ± 1.306	0.268	0.792	(113) 15.28 ± 0.500	(28) 17.11 ± 1.131	(85) 14.68 ± 0.539	2.126	0.0357
Fitness relative to N2	(9) 1.000 ± 0.117	(10) 0.095 ± 0.021	8.015	< 0.0001	(113) 0.290 ± 0.027	(28) 0.400 ± 0.039	(85) 0.254 ± 0.033	2.333	0.0214
Fitness relative to *gas*-1 G0	(9) 7.026 ± 0.736	(10) 1.000 ± 0.195	8.305	< 0.0001	(113) 2.584 ± 0.196	(28) 3.541 ± 0.300	(85) 2.269 ± 0.232	2.891	0.0046
Unhatched eggs	(9) 1.222 ± 0.401	(10) 4.000 ± 1.333	1.903	0.0741	(113) 1.973 ± 0.193	(28) 1.571 ± 0.269	(85) 2.106 ± 0.240	1.199	0.2333
Bagging	3/9	1/10	—	0.3034	44/113	8/28	36/85	—	0.2645

Sample sizes are shown in parentheses; other values are means ± 1 SEM. Two-tailed Student's *t*-test statistics and associated *P*-values are shown comparing *gas-1* G0 and N2, and male RC lines with no-male RC lines. Bagging denotes the fraction of bagging hermaphrodites. Fisher's exact test *P*-value reported comparing *gas-1* G0 and N2, and male RC lines with no-male RC lines for this trait. RC, recovery.

outcrossing rates (± 1 SEM) were 0.195 (0.057) for the N2 × *gas-1* G0 control cross, 0.434 (0.051) for high-male RC lines × N2, and 0.099 (0.051) for no-male RC lines × N2. The average fraction of male offspring (± 1 SEM) from the same crosses—expected to be 50% with all outcross progeny—mirrored the outcrossing results with 0.098 (0.029) for N2, 0.217 (0.026) for high-male, and 0.050 (0.026) for no-male RC lines. The total number of offspring produced by each strain and RC line in these assays corresponded to the results of the conventional fitness assays. During these experiments, we also observed that hermaphrodites from no-male RC lines demonstrated a high latency to mate compared to hermaphrodites from high-male RC lines. The few successful crosses conducted between *gas-1* G0 males and RC line hermaphrodites were consistent with this result not being a consequence of N2 male mating strategy; no-male RC line hermaphrodites were poor outcrossers regardless of male strain.

Life history evolution of gas-1 RC lines

After 60 generations of evolution in large, nonoverlapping populations, neither absolute fitness, *W*, nor relative fitness of the *gas-1* RC lines improved significantly over *gas-1* G0 on average (Table 1 and Table S2). However, there was significant among-RC line variability in evolutionary response (Figure 1, Figure 2, and Figure 3), with two distinct classes of lines emerging: a low-fitness class whose reproductive schedule was still similar to that of *gas-1* G0 after 60 generations and a high-fitness class (Figure 1). Seven lines (RC3, RC8, RC9, RC10, RC13, RC20, and RC22) had significantly higher *W* than *gas-1* G0 (Dunnett's test, $P < 0.05$). The same lines, in addition to RC12 and RC18, had significantly higher fitness relative to *gas-1* G0. The *gas-1* RC lines showing significant improvements for absolute and relative fitness largely overlap those noted as generating appreciable numbers of males (Figure 1) or evolving bleach resistance. No RC lines in the lower-fitness class were noted to contain males. There was no difference among mean N2, *gas-1* G0, or *gas-1* RC line life span; however, there was a weakly significant tendency for high-male lines to live longer than no-male lines (Table 1). Finally, there were no significant differences, either between strains (*gas-1* RC *vs.* *gas-1* G0) or among *gas-1* RC lines, in the presence of unhatched eggs, or the prevalence of "bagging" (internal hatching of eggs), even when the presence of males was taken into account (Table 1).

Comparison of relative and competitive fitness

Mean levels of relative and competitive fitness of individual strains were positively correlated (Spearman's $\rho = 0.6294$, $P = 0.0090$), although the distribution of competitive fitness values was rather bimodal, failing to distinguish strains to the same extent as relative fitness (Figure 3, and Figures S1 and S2). The *gas-1* G0 control performed worse than all but one *gas-1* RC line tested in competition against the GFP-marked strain, while N2 performed best. No strain outcompeted the GFP-marked strain, although eight RC lines competed at levels > 70% of the GFP tester strain. The *gas-1* RC lines noted as generating high frequencies of males (Figure 3, purple symbols) tended to perform better in both types of fitness assays than those without males, but performed especially well in the competitive fitness assays. With two exceptions (RC7 and RC11), most lines scoring low on relative fitness cluster about the origin, suggesting that differences in strain performance in the two types of assays are mainly realized for lines expressing higher relative fitness.

Evolution of ROS levels

As previously observed (Christy *et al.* 2017), *gas-1* G0 exhibited significantly higher ROS levels than N2 (Figure 4). Of the four gas-1 RC lines assayed, ROS levels were significantly reduced compared with *gas-1* G0 and mostly statistically indistinguishable (although mostly lower) than wild-type levels. Line RC2, which exhibited higher ROS levels than the other RC lines, scored far lower in both relative and competitive fitness assays than the other lines assayed.

Changes in mtDNA copy number

As previously reported from an independent data set (Wernick *et al.* 2016), relative mtDNA copy number (mtDNA coverage normalized by coverage at single-copy nuclear regions) was

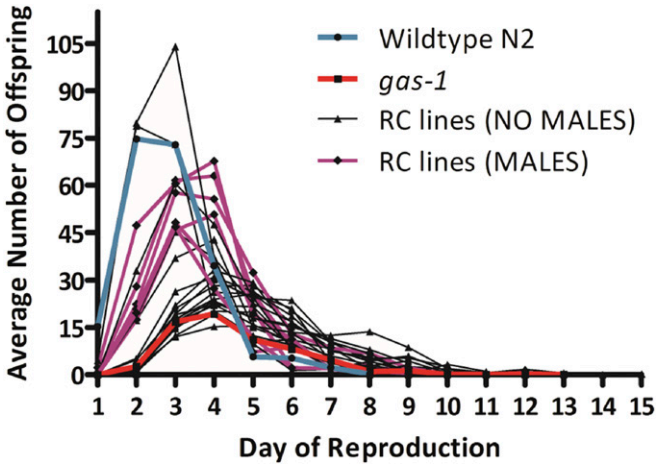

Figure 1 Reproductive schedules of *gas-1* recovery (RC) lines. Average daily productivity of G60 *gas-1* RC lines alongside that of their *gas-1* ancestor (red line) and wild-type N2 (blue line) controls. The six RC lines that evolved appreciable frequencies of males are highlighted in purple. Line RC10 and the bleach-resistant line, RC22, exceeded wild-type peak reproduction.

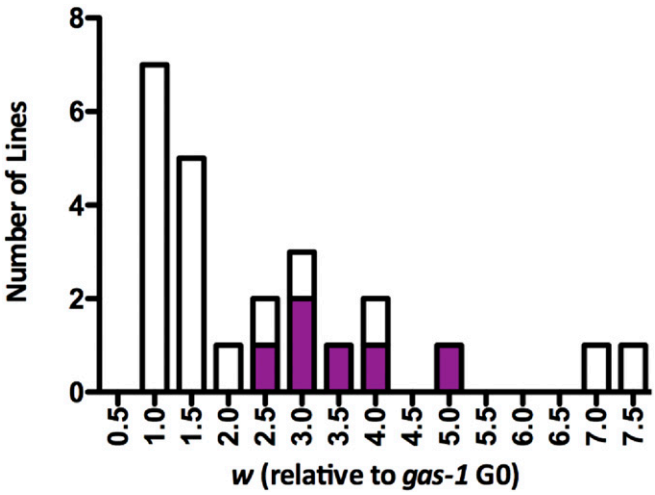

Figure 2 Frequency histogram of gas-1 recovery (RC) line relative fitness. Histogram of the 24 *gas-1* RC lines' fitness (*w*) relative to *gas-1* G0 (equal to 1.0). Filled portions of bars indicate contribution of male-containing RC lines.

not different between the N2 and *gas-1* progenitor strains (120.6× and 128.2×, respectively). A Levene's test determined the *gas-1* RC lines had unequal variance (F_{23} = 1.9838, $P < 0.0001$) with respect to mtDNA copy number (Figure S3 and Table S3). Using normalized mitochondrial DNA coverage for 12 mitochondrial genes and two ribosomal sequences in N2, *gas-1* G0, and the 24 RC lines, the analysis determined that strain was a significant factor (Kruskal–Wallis $H = 288.72$, $P < 0.0001$). Kruskal multiple comparison *post hoc* tests evaluated the significance of normalized mtDNA copy number among pairwise comparisons of all lines. Five of the 24 *gas-1* RC lines showed significant increases in relative mtDNA copy number compared to *gas-1* G0—RC7, RC8, RC9, RC10, and RC11—while the remaining 19 lines showed no difference. The average normalized mtDNA copy number of *gas-1* RC lines was 157.7×, ~1.23 times higher than *gas-1* G0. Coverage patterns across sites were consistent among lines (Figure S3), indicating that complete mitogenome copy number had increased rather than isolated sections of the mitochondrial genome.

Reversion of background mutations in gas-1 G0

As previously described, bioinformatic analysis of our *gas-1* G0 strain revealed the presence of 76 mutations in addition to the *gas-1(fc21)* mutant allele compared to our N2 lab reference strain, even following 10 generations of backcrossing to N2 [Table S2 in Christy *et al.* (2017)]. The majority of these were G: C→A: T transitions, consistent with the original *gas-1* mutant having been derived from an EMS mutagenesis screen. The X-chromosome (where *gas-1* is located) harbored the majority, 62%, of such mutations. While all 76 background mutations were retained within the previously analyzed *gas-1* MA lines derived from *gas-1* G0 (Christy *et al.* 2017), we discovered that four of these 76 mutations had reverted to the wild-type allele within individual generation-60 RC lines (Table S4). There were no reversions of the ancestral *gas-1(fc21)* allele. Three of these SNPs were reverted in three different RC lines, each belonging to the lower-fitness class and not noted to have high male frequency. These included substitutions in introns of genes residing on chromosomes V and X (Y17D7C.2 and *ceh-37*, respectively), and a synonymous substitution in the *emc-2* gene of chromosome II. None of these genes have known involvement in sex determination, dosage compensation, chromosome dynamics, or mating behavior. Interestingly, the fourth mutation, residing within an intron of the *fox-1* gene, reverted to the wild-type nucleotide in three RC lines (RC3, RC12, and RC24), belonging to the higher-fitness class of RC lines and noted as having evolved high male frequency during the experiment. *Fox-1*, distantly located (> 13 Mb) from *gas-1* on the X chromosome, is an RNA-binding protein involved in early-embryo dosage compensation and male mating behavior (Skipper *et al.* 1999).

mtDNA single-base substitutions

A total of 392 mtDNA single-base pair variants were identified, the majority (n = 317) of which were located within the AT-rich region (~13,327–13,794 bp) and had low coverage (1–3×) of the variant nucleotide. Another 59 variants failed to meet the required coverage for the candidate site and/or the variant nucleotide (6×). After filtering, 16 candidates remained. Three of the 16 were identified within our N2 lab strain (*i.e.*, differences between our lab strain and the N2 reference), while 13 unique mutations were distributed among *gas-1* RC lines (Table S5). A review of the mtDNA positions in which one of these 13 unique mutations was identified revealed no convincing evidence of their existence within N2, other RC lines, or previously analyzed *gas-1* MA lines. Specifically, frequencies of the base calls for these

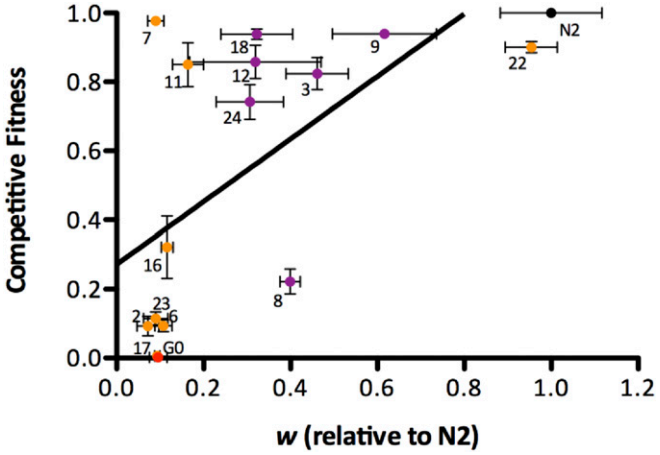

Figure 3 Relationship between relative and competitive fitness. Data points represent a subset of *gas-1* recovery (RC) lines along with *gas-1* G0 (red symbol) assayed for fitness relative to N2 (black symbol) and competitive fitness with a GFP-marked strain. Orange symbols indicate *gas-1* RC lines without evidence for males; purple symbols indicate *gas-1* RC lines in which the presence of males was noted (note that RC10 was not among the lines sampled for competitive fitness assays; Figures S1 and S2 show complete data for relative and competitive fitness, respectively). Error bars = 1 SEM. The black line indicates the best-fit line of the data using standard least squares regression. where y is competitive fitness and x is relative N2 fitness: $y = 0.819(x) + 0.286$ ($F_{1,\ 14} = 8.192$, $P = 0.0125$, nonsignificant intercept).

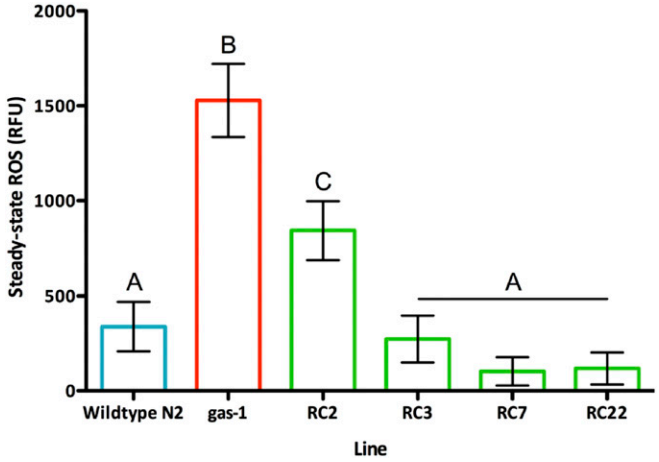

Figure 4 Steady-state reactive oxygen species (ROS) levels. ROS levels (mean ± 1 SEM) for N2 (338.7 ± 127.0), *gas-1* G0 (1527.8 ± 154.4), and four selected recovery (RC) lines at generation 60 of recovery: RC2 (843.6 ± 117.1), RC3 (273.7 ± 125.2), RC7 (102.7 ± 105.8), and RC22 (118.8 ± 128.9). Lines differed with regard to ROS ($F_{5,208} = 16.01$, $P < 0.0001$); *gas-1* G0 had significantly higher ROS content than N2 and the four *gas-1* RC lines (Tukey's honest significant difference, $\alpha = 0.05$). Error bars = 1 SEM and letters label statistically indistinguishable groups. RC2 and RC7 were members of the lower-relative fitness class, although RC7 scored high in competitive fitness. RC22 and RC3 were members of the higher-fitness class (Figure 1). RC22 evolved bleach resistance; RC3 evolved high-male frequency. RFU, relative fluorescence unit.

mutations within other RC lines (File S1) and previously analyzed *gas-1* MA lines (File S2) mostly fall < 0.001, far below what we would consider to be indicative of a candidate mutation rather than a result of sequencing error, estimated at 0.1% for Illumina HiSeq (Fox *et al.* 2014). If any of these variants is real, it is also possible that they reflect somatic variants segregating in one or two individuals in the sequenced population. Of the 13 RC line-specific mutations, four were present at levels of > 99% in the sample and were thus likely to be homoplasmic; the remaining were variable, detected at levels ranging from 2.5 to 95%. Three RC lines (RC3, RC13, and RC19) contained two substitutions each; the other seven contained single substitutions. Apart from two substitutions, one each in a tRNA and an rRNA gene, variants were discovered within protein coding genes (Figure S4 and Table S5). All but two were amino acid replacing. Figure S4 shows the observed percentage of RC line mutations discovered in *nduo-6* and *nduo-1*, which exceed three and two SD of the mean expected percentages, respectively (see File S3 for simulation code). Notably, RC lines containing mtDNA mutations exhibited considerable parallel evolution. Lines RC5 and RC22 acquired the same nonsynonymous substitution within the *nduo-1* gene, while lines RC13, RC18, and RC24 acquired the same nonsynonymous substitution within the *nduo-6* gene. Except for that in RC5, these changes were nearly or completely homoplasmic (Table S5).

An extremely rough estimate of the number of times we could expect any particular mitochondrial site to be mutated (not fixed for a new substitution) in our experiment is given by: the *C. elegans* mitochondrial base substitution mutation rate (4.32 × 10–8 per site per generation; Konrad *et al.* 2017) × the approximate N_e for the RC line mitochondria (62,000) × the number of generations of evolution (60) × the number of experimental lines (24) = 3.856, matching the number observed for the G→T substitution at position 227 of the *nduo-6* locus (Table S5). The true N_e for this experiment is difficult to judge; however, the chance of multiple independent observations of a particular mutation is far more likely in the mitochondrial than in the nuclear genome owing to the higher mutation rate and N_e of mtDNA, with the latter estimated at 62 for *C. elegans* (Konrad *et al.* 2017). This calculation suggests that parallel mtDNA evolution is well within the realm of possibility. Furthermore, transgenerational PCR surveys of two RC line base substitutions (the G→T change in the *nduo-1* gene of RC18 and the C→T change in the *nduo-6* gene of RC22; Figure S5) show the trajectory of each mutation through a period of heteroplasmy or polymorphism (*i.e.*, both mutant and wild-type bases present in the sequenced population of scores of L1 offspring collected directly from frozen RC line stocks) toward eventual fixation.

gas-1 RC line nuclear mutations

Nuclear mutations in the 24 sequenced *gas-1* RC lines were identified and bioinformatically characterized as before (Christy *et al.* 2017). A total of 111 nuclear genome SNPs was detected; of these, 28 occurred in introns, 18 in exons, 62 mutations were intergenic, and 3 occurred in pseudogenes

(Table S6). Of the 18 exonic SNPs, 7 were synonymous and 11 were nonsynonymous. RC line-specific mutation numbers ranged from 1 (in RC14, RC15, and RC21) to 11 (in RC13). As observed for both *gas-1* MA lines (Christy *et al.* 2017) and N2 MA lines (Denver *et al.* 2012), G:C → A:T transitions were the most common substitution type encountered in *gas-1* RC lines (36/111), followed by A:T → T:A transversions. The rank order of the remaining four mutation types was also comparable between *gas-1* RC and published MA values, with the least common mutation events—9/111—being A:T → C:G transversions. None of the 111 were in known mitochondria-targeted genes.

GO term enrichment

File S4 gives a complete account of *gas-1* RC G0 enrichment results. Four GO slim categories were significantly enriched in the *gas-1* RC lines: the biological processes of cell organization and biogenesis, cytoskeleton organization and biogenesis, protein modification, and the molecular function category of phosphoprotein phosphatase activity (Figure S6A). Although not significantly enriched, likely due to the very large number of gene annotations contained within each GO term category, large numbers of *gas-1* RC line SNPs mapped to several other categories including reproduction and metabolic process (Figure S7). Overlapping sets of RC line mutated genes mapped to each of the four aforementioned categories. Ten *gas-1* RC line mutated genes mapped to the cell organization and biogenesis term: *ttn-1*, *syd-2*, *slt-1*, *tir-1*, *fer-1*, *ppfr-1*, *math-33*, *ced-12*, *Y34B4A.2*, and *pph-4.1*; four to cytoskeleton organization and biogenesis: *ttn-1*, *ppfr-1*, *ced-12*, and *pph-4.1*; nine to protein modification: *ttn-1*, *tir-1*, *C17H12.3*, *Y54F10BM.3*, *ppfr-1*, *Y106G6D.4*, *math-33*, *pph-4.1*, and *set-29*; and three to phosphoprotein phosphatase activity: *Y54F10BM.3*, *pph-4.1*, and *C17H12.3*. Among the 14 unique genes in this set, several have fertility and embryogenesis functional annotations (Figure S7). Functional analysis of the *gas-1* G0 interactome gene set (Christy *et al.* 2017) revealed shared enrichment of the three biological process categories that were enriched in the *gas-1* RC lines: cell organization and biogenesis, cytoskeleton organization and biogenesis, and protein modification; however, the molecular function category of phosphoprotein phosphatase activity was not significantly enriched in the *gas-1* interactome gene set. Conversely, no enriched G0 slims were shared between the *gas-1* RC and previously reported MA line [figure 3a in Christy *et al.* (2017)] gene sets.

gas-1 interactions

Of the 46 genic mutations (*i.e.*, those discovered within exons or introns) found within sequenced *gas-1* RC lines, 13 were predicted to interact within two degrees of the *gas-1* gene (Figure S6B and Table S7). Note that two distinct mutations were observed within the mitochondrial *nad-1* gene at positions 1977 and 2154 bp, totaling 13 mutations in 12 genes that exhibit interactions within two degrees of *gas-1*. One of these, *nad-1*—encoding mitochondrial NADH dehydrogenase subunit I—was a direct interactor with *gas-1*. *nduo-6*, encoding another subunit of the same complex, is also predicted to directly interact with the *gas-1* gene; however, its interaction value (2.05) did not meet the threshold of 4.5. By contrast, none of the 76 *gas-1* G0 background mutations were found within the interactome. This is not especially surprising since these mutations, far from being a random sample of spontaneous substitutions, are all linked (the majority physically linked on the X chromosome) to *gas-1*. Of 59 genic mutations found within sequenced N2 MA lines (Christy *et al.* 2017), 12 were located within the *gas-1*-centric interactome.

Discussion

Evolution of male frequency accompanies fitness recovery

We found that evolution, under conditions of large population size and competition for food resources, could at least partly recover ancestral fitness and phenotypes on this short timescale. Two distinct fitness classes of G60 RC lines emerged (Figure 1 and Table 1); the one exhibiting greater fitness gains contained lines that evolved resistance to bleach treatment or high male frequencies during the experiment. Reversion of a *fox-1* background mutation within three high-male, high-fitness RC lines (Table S4) may have provided one route to the evolution of male frequency. However, this reversion cannot fully explain the evolution of male frequency since wild-type laboratory populations of *C. elegans* N2 generate only ~0.1% males; perhaps the intronic *fox-1* mutation within the *gas-1* G0 ancestor stifled the evolution of males in RC lines that did not experience reversion to wild-type. No other candidate sexual modifier mutations emerged from our analysis; the genetic basis for male frequency evolution in our lines thus remains unknown. High-male RC lines tended to perform especially well when fitness was measured in competition (Figure 3). Together with our finding that rates of chromosome nondisjunction were no different in high- *vs.* no-male RC lines, this observation is consistent with the prediction that adaptation is facilitated by recombination.

It is important to note that our observations of male frequency were anecdotal and incomplete. Other RC lines may have generated low frequencies of males that escaped observation. Furthermore, we failed to quantify male frequency until after the lines had been cryogenically stored. The inability to recover appreciable frequencies of males from these RC lines under benign conditions is consistent with males having been selectively favored under our specific evolution regime. Indeed, laboratory *C. elegans* populations exposed to selection have been observed to maintain males at significantly higher frequencies than wild-type N2 (Anderson *et al.* 2010; Teotonio *et al.* 2012); we therefore do not believe that the evolution of male frequency in our lines is specific to *gas-1*. It is possible that the bleach age synchronizations performed between each recovery generation or some other

aspect of our treatment constituted an appropriate selective agent. Results of the mating assays are consistent with both male mating ability, and hermaphrodite outcrossing ability and latency to mate, having been targets of selection. In summary, our analyses cannot discern whether male frequency and outcrossing rates were causes or consequences of fitness evolution; future work will explore this issue in a controlled manner.

Recovery of ROS levels and generalized upward evolution of mtDNA copy number

Based on the subset of lines assayed, laboratory adaptation in *gas-1* RC lines appeared to have been accompanied by evolution of lower steady-state ROS levels (Figure 4), which could result from lower ROS production or improved scavenging. In support of this idea, the line exhibiting highest G60 ROS, RC2, was a no-male line that scored low in both types of fitness assay. Recovery of ancestral ROS levels suggests that laboratory adaptation of *gas-1* lines involved restoration of mitochondrial function. RC line evolution was also accompanied by increased mtDNA copy number in nearly all lines, with roughly 20% exhibiting a statistically significant increase over *gas-1* G0 and N2 controls (Figure S3). Elevated mtDNA levels could have provided a route to fitness recovery through compensatory effects on mitochondrial function. Interestingly, however, a magnified pattern of increasing mtDNA levels was previously measured for MA lines initiated from both *gas-1* and wild-type N2, and evolved under genetic drift (Wernick *et al.* 2016). In the current study, the increase in average mtDNA copy number of *gas-1* RC lines compared to *gas-1* G0—∼1.23×—was substantially lower than that observed for G43 *gas-1* MA lines, which ranged from 2.2 to 3.4 times higher than *gas-1* G0. In summary, while increased mtDNA levels in RC lines may be adaptive, a neutral or potentially maladaptive scenario seems more likely. Indeed, the five *gas-1* RC lines showing statistically significant gains in mtDNA levels were not distinguished by their high fitness levels, but rather were members of both high- and low-fitness classes.

nDNA evolution and signatures of positive selection

Whole-genome analysis of the 24 *gas-1* RC lines discovered 111 nDNA single-base substitutions (1–11 per line) and no reversions of the ancestral *gas-1(fc21)* allele. Thus, all phenotypic evolution within *gas-1* RC lines resulted from secondary mutations. There was no correlation between RC line-specific means of any measured phenotype and the number of any SNP type, *e.g.*, exonic or nonsynonymous. As the overall numbers of SNPs occurring in exon sequences was small ($n = 18$; Table S6), a d_N/d_S analysis could not be performed. Although we believe it to be unlikely, we acknowledge that reversion of background mutations fixed within the *gas-1* G0 ancestor (Table S4) or compensations for any deleterious effects of these mutations could have provided a means of fitness recovery for six lines. Apart from the three *fox-1* reversions occurring within three high-fitness RC lines, there was no correlation between the other three such reversions and G60 fitness. While the likelihood that the *fox-1* reversions arose independently is small, we have observed evidence of parallel nDNA substitutions in experimental lines evolving under similar conditions on this timescale before (Denver *et al.* 2010), consistent with findings that population size (rather than genome size, etc.) may be the main driver of parallel genome evolution in evolve-and-resequence studies (Bailey *et al.* 2017). While reversions of unassayed mutation types (*e.g.*, insertion/deletions) could also have contributed to RC line fitness evolution, the EMS treatment employed to generate the original *gas-1* mutant generates ∼99% G:C→A:T transitions (Greene *et al.* 2003; Kim *et al.* 2006); our mutation analysis was thus unlikely to have missed important contributors.

Results of interactome analyses (Figure S6 and Table S7) bore the signature of positive selection, demonstrating that many fixed RC line SNPs mapped to the *gas-1*-centric interactome. Approximately one-quarter of all mutations occurred in genes interacting within two degrees from *gas-1*, a potential indicator of compensatory evolution (notably, none of the background mutations fixed within *gas-1* G0 are in loci predicted to interact within two degrees of *gas-1*, *i.e.*, they are unlikely to be hidden targets of compensatory evolution). However, it is worth noting that 20% (12/59) of mutations previously discovered in the *gas-1* MA lines also fell within the *gas-1*-centric network. While this fraction was no different from that expected by chance, it does not differ substantially from the *gas-1* RC line result.

Many of the same SNPs mapped to GO terms found to be significantly enriched: two biogenesis and organizational categories along with protein modification, and phosphoprotein phosphatase (Figure S7 and File S4). For instance, *pph-4.1*, encoding a protein phosphatase subunit necessary for proper centrosome functioning and meiotic chromosome dynamics (Sumiyoshi *et al.* 2002; Sato-Carlton *et al.* 2014), acquired an intronic mutation that appears in the *gas-1*-centric interactome (Figure S6B), where it interacts with a histone deacetylase gene, *hda-1* (Table S7), and maps to all four significantly enriched GO terms (Figure S7). Several RC line SNPs were annotated as being involved in fertility-related processes (File S4). These results contrast with analyses of the *gas-1* MA lines (Christy *et al.* 2017); these lines contained more mutations that the *gas-1* RC lines, but had fewer significantly enriched GO slims (*i.e.*, plasma membrane and transport), in agreement with the idea that less defined evolutionary pathways lead to fitness decline under drift than to fitness recovery under selection. A caveat is that the GO term analysis package we used does not account for differences in the lengths of genes annotated to different GO terms, which could have influenced these comparisons (Kofler and Schlotterer 2012).

Evidence for mitonuclear adaptation

Our most compelling evidence for adaptive mutation in RC lines comes from the analyses of mtDNA genomes (Table S5).

Thirteen variants were discovered: five homoplasmic (fixed) and eight variable. Although we cannot know with certainty whether these mutations arose *de novo* during the experiment or instead were present within the single *gas-1* G0 ancestral individual at low heteroplasmy levels, our failure to find convincing evidence of these variants in the ancestral strain, any other RC line, or previously studied *gas-1* MA lines supports the idea that they are novel. It is also worth noting that cryptic paralogy is far less problematic for mtDNA than for nDNA resequencing projects. A large fraction (7/13) of these variants caused amino acid replacements in two ETC complex I proteins, ND1 and ND6 (Figure S4), with the former predicted to physically interact with the nuclear-encoded GAS-1 protein (Figure S6B). We also found evidence of considerable parallel evolution with two of these mutations discovered in two and three RC lines, respectively. Neither the results of our *gas-1* MA experiment (Wernick *et al.* 2016) nor those from wild-type MA lines (Konrad *et al.* 2017) suggest that these sites are hotspots for mutation. Two RC lines in which these mtDNA mutations were detected as segregating variants were members of the low-fitness class. Conversely, four of the five lines in which these mutations were detected as nearly or completely homoplasmic were members of the high-fitness class; three of these five were members of the high male frequency class. One of the aforementioned lines was RC22, whose mtDNA differed from that of wild-type N2 by a single nucleotide causing an S→L replacement in the ND1 protein (Table S5). This line exhibited the greatest recovery of wild-type reproductive and competitive fitness (Figure 3), and evolved resistance to the bleach treatments used to synchronize lines each generation; however, no males were detected in this line. Line RC10, which exhibited the second-greatest fitness gains, was also not noted to contain males, suggesting that outcrossing was not a prerequisite of rapid adaptation.

nduo-1 and *nduo-6* interface between the hydrophobic membrane arm and the hydrophilic matrix arm of complex I, in which the GAS-1 subunit is located (Brandt 2006; Efremov and Sazanov 2011; Sazanov 2015). GAS-1 is the immediate electron donor to ubiquinone and helps to form the quinone-binding pocket of complex I (Vasta *et al.* 2011; Shiraishi *et al.* 2012). Several studies suggest that *nduo-1* also contributes to ubquinone binding (Darrouzet *et al.* 1998; Kurki *et al.* 2000; Brandt 2006). Although *nduo-6* is not known to participate directly in ubiquinone binding, it may contribute to the interaction between complex I and ubiquinone (Jun *et al.* 1996; Pätsi *et al.* 2008). We hypothesize that the *nduo-1* and *nduo-6* mutations discovered within RC lines partially ameliorate the reduced complex I activity caused by the *gas-1* mutation. Individual characterization of these candidate adaptive mutations will be reported elsewhere.

Conclusions

We found that ETC mutant lineages can partially recover wild-type fitness levels via fixation of novel mutations on a short evolutionary timescale, and that many of the causal mutations are likely to cluster within the same functional network as the original mutant allele. The evolution of outcrossing appeared to accompany such fitness recovery, especially for RC lines that fixed particular mtDNA mutations. Our finding that fixation of mtDNA mutations may have facilitated the rapid adaptation of certain *gas-1* RC lines would provide the first direct evidence for adaptive, compensatory mtDNA mutation-driven evolution.

The same observations that spawned the previously mentioned nuclear compensation hypothesis (Osada and Akashi 2012; Burton *et al.* 2013) also led to the formation of a new hypothesis to explain the evolution and maintenance of sexual reproduction: the mitonuclear sex hypothesis (Havird *et al.* 2015a). Both hypotheses are predicated on the assumption that mtDNA genomes experience ongoing genomic decay, a topic of much debate. Described as a "Red Queen hypothesis with a mitonuclear twist" (Hill 2015), the mitonuclear sex hypothesis suggests that sex is maintained because it increases the rate at which new combinations of nDNA alleles able to compensate the theoretically ongoing mtDNA genome decay are introduced into populations. Similar benefits would not extend to asexually propagating mtDNA, where adaptive mutation dynamics are expected to be strongly influenced by clonal interference. It further predicts that, in facultatively outcrossing lineages, sex will be favored in cases of mitonuclear mismatch. Our results do not appear to provide especially strong support for either of the above hypotheses. While mitonuclear mismatch may have promoted outcrossing in some of our lines, we observed that fixation of mtDNA and nDNA (rather than only nDNA) mutations may have been key facilitators of rapid adaptation in *gas-1* RC lines, and that lines fixing mtDNA mutations were those with the strongest tendency to evolve high outcrossing rates. However, the fact that we generated RC lines only from one nDNA mutant leaves ample room for question.

Our study may have nonetheless exposed a case in which mtDNA- rather than nDNA-driven mitonuclear adaptation is promoted by sexual recombination; *i.e.*, one of extreme mitonuclear mismatch and associated reduction in fitness. Here, outcrossing would generate different combinations of new mitotypes (supplied by the high rate of mtDNA mutation) and *gas-1* mutation-bearing nDNA backgrounds, thereby promoting rapid fixation of compensatory mtDNA mutations. Furthermore, because our lines evolved from a genetically invariant ancestor, they would be unlikely to suffer from outcrossing-induced recombination load resulting from the breakup of beneficial allelic combinations (Whitlock *et al.* 2016). Outcrossing might easily invade selfing populations under such circumstances, analogous to situations described by "class I models" for the evolution of sex defined by Sharp and Otto (2016). These models include Red Queen and Spatial Heterogeneity models, in which sex serves to break up previously beneficial but currently obsolete allelic combinations. Our experiment generated an intergenomic version of this scenario by forcing mitonuclear mismatch. Whether such a process has a bearing for populations with less extreme mitonuclear match where selection would be less intense,

or in more genetically heterogeneous populations wherein sex might also serve to break up beneficial mitonuclear combinations (Radzvilavicius 2016), inducing a recombination load, is completely unstudied. Furthermore, short-term costs of breaking apart allelic combinations built by previous selection can, in certain cases, impede the invasion of sexual modifiers (*e.g.*, Otto and Feldman 1997). There is clearly much to learn about the forces shaping mitonuclear coevolution. The complexity of mitochondrial population dynamics and our incomplete understanding of the relative influence of evolutionary forces acting on mtDNA genomes imply that this is an ideal problem for the application of experimental evolution and population genomics (c.f., McDonald *et al.* 2016).

Acknowledgments

We thank A. Basler and L. Muñoz Tremblay for laboratory support, the P.C. Phillips group (University of Oregon) for helpful discussion, and A. Agrawal and two anonymous reviewers for insightful comments. We also thank the Oregon State University Center for Genome Research and Biocomputing for DNA sequencing and bioinformatics support. This work was supported by the National Science Foundation (MCB-1330427 to S.E. and D.R.D., and HRD-140465 to S.E., which supported the undergraduate research of J.F.R.) and the Portland State University Biology Department (Forbes-Lea grant to S.F.C.).

Literature Cited

Alexeyev, M., I. Shokolenko, G. Wilson, and S. LeDoux, 2013 The maintenance of mitochondrial DNA integrity–critical analysis and update. Cold Spring Harb. Perspect. Biol. 5: a012641. https://doi.org/10.1101/cshperspect.a012641

Anderson, J. L., L. T. Morran, and P. C. Phillips, 2010 Outcrossing and the maintenance of males within C. elegans populations. J. Hered. 101: S62–S74. https://doi.org/10.1093/jhered/esq003

Arnqvist, G., D. K. Dowling, P. Eady, L. Gay, T. Tregenza *et al.*, 2010 Genetic architecture of metabolic rate: environment specific epistasis between mitochondrial and nuclear genes in an insect. Evolution. 64: 3354–3363. https://doi.org/10.1111/j.1558-5646.2010.01135.x

Azevedo, L., J. Carneiro, B. van Asch, A. Moleirinho, F. Pereira *et al.*, 2009 Epistatic interactions modulate the evolution of mammalian mitochondrial respiratory complex components. BMC Genomics 10: 266. https://doi.org/10.1186/1471-2164-10-266

Bailey, S. F., F. Blanquart, T. Bataillon, and R. Kassen, 2017 What drives parallel evolution?: How population size and mutational variation contribute to repeated evolution. Bioessays 39: 1–9. https://doi.org/10.1002/bies.201600176

Ballard, J. W., and M. C. Whitlock, 2004 The incomplete natural history of mitochondria. Mol. Ecol. 13: 729–744. https://doi.org/10.1046/j.1365-294X.2003.02063.x

Barreto, F. S., and R. S. Burton, 2013 Evidence for compensatory evolution of ribosomal proteins in response to rapid divergence of mitochondrial rRNA. Mol. Biol. Evol. 30: 310–314. https://doi.org/10.1093/molbev/mss228

Bazin, E., S. Glémin, and N. Galtier, 2006 Population size does not influence mitochondrial genetic diversity in animals. Science 312: 570–572. https://doi.org/10.1126/science.1122033

Bergstrom, C. T., and J. Pritchard, 1998 Germline bottlenecks and the evolutionary maintenance of mitochondrial genomes. Genetics 149: 2135–2146.

Brandt, U., 2006 Energy converting NADH:quinone oxidoreductase (complex I). Annu. Rev. Biochem. 75: 69–92. https://doi.org/10.1146/annurev.biochem.75.103004.142539

Burton, R. S., R. J. Pereira, and F. S. Barreto, 2013 Cytonuclear genomic interactions and hybrid breakdown. Annu. Rev. Ecol. Evol. Syst. 44: 281–302. https://doi.org/10.1146/annurev-ecolsys-110512-135758

Christy, S. F., R. I. Wernick, M. J. Lue, G. Velasco, D. K. Howe *et al.*, 2017 Adaptive evolution under extreme genetic drift in oxidatively stressed *Caenorhabditis elegans*. Genome Biol. Evol. 9: 3008–3022. https://doi.org/10.1093/gbe/evx222

Cooper, B. S., C. R. Burrus, C. Ji, M. W. Hahn, and K. L. Montooth, 2015 Similar efficacies of selection shape mitochondrial and nuclear genes in both Drosophila melanogaster and Homo sapiens. G3 (Bethesda) 5: 2165–2176.

Darrouzet, E., J.-P. Issartel, J. Lunardi, and A. Dupuis, 1998 The 49-kDa subunit of NADH-ubiquinone oxidoreductase (Complex I) is involved in the binding of piericidin and rotenone, two quinone-related inhibitors. FEBS Lett. 431: 34–38. https://doi.org/10.1016/S0014-5793(98)00719-4

Denver, D. R., K. Morris, M. Lynch, L. L. Vassilieva, and W. K. Thomas, 2000 High direct estimate of the mutation rate in the mitochondrial genome of *Caenorhabditis elegans*. Science 289: 2342–2344. https://doi.org/10.1126/science.289.5488.2342

Denver, D. R., P. C. Dolan, L. J. Wilhelm, W. Sung, J. I. Lucas-Lledó *et al.*, 2009 A genome-wide view of *Caenorhabditis elegans* base-substitution mutation processes. Proc. Natl. Acad. Sci. USA 106: 16310–16314. https://doi.org/10.1073/pnas.0904895106

Denver, D. R., D. K. Howe, L. J. Wilhelm, C. A. Palmer, J. L. Anderson *et al.*, 2010 Selective sweeps and parallel mutation in the adaptive recovery from deleterious mutation in Caenorhabditis elegans. Genome Res. 20: 1663–1671. https://doi.org/10.1101/gr.108191.110

Denver, D. R., L. J. Wilhelm, D. K. Howe, K. Gafner, P. C. Dolan *et al.*, 2012 Variation in base-substitution mutation in experimental and natural lineages of Caenorhabditis nematodes. Genome Biol. Evol. 4: 513–522. https://doi.org/10.1093/gbe/evs028

de Paula, W. B., A. N. Agip, F. Missirlis, R. Ashworth, G. Vizcay-Barrena *et al.*, 2013 Female and male gamete mitochondria are distinct and complementary in transcription, structure, and genome function. Genome Biol. Evol. 5: 1969–1977. https://doi.org/10.1093/gbe/evt147

Dowling, D. K., A. L. Nowostawski, and G. Arnqvist, 2007 Effects of cytoplasmic genes on sperm viability and sperm morphology in a seed beetle: implications for sperm competition theory? J. Evol. Biol. 20: 358–368. https://doi.org/10.1111/j.1420-9101.2006.01189.x

Dowling, D. K., U. Friberg, and J. Lindell, 2008 Evolutionary implications of non-neutral mitochondrial genetic variation. Trends Ecol. Evol. 23: 546–554. https://doi.org/10.1016/j.tree.2008.05.011

Efremov, R. G., and L. A. Sazanov, 2011 Structure of the membrane domain of respiratory complex I. Nature 476: 414–420. https://doi.org/10.1038/nature10330

Ellison, C. K., and R. S. Burton, 2006 Disruption of mitochondrial function in interpopulation hybrids of *Tigriopus californicus*. Evolution 60: 1382–1391. https://doi.org/10.1111/j.0014-3820.2006.tb01217.x

Estes, S., and M. Lynch, 2003 Rapid fitness recovery in mutationally degraded lines of *Caenorhabditis elegans*. Evolution 57: 1022–1030. https://doi.org/10.1111/j.0014-3820.2003.tb00313.x

Estes, S., P. C. Phillips, D. R. Denver, W. K. Thomas, and M. Lynch, 2004 Mutation accumulation in populations of varying size: the distribution of mutational effects for fitness correlates in

Caenorhabditis elegans. Genetics 166: 1269–1279. https://doi.org/10.1534/genetics.166.3.1269

Estes, S., A. L. Coleman-Hulbert, K. A. Hicks, G. de Haan, S. R. Martha *et al.*, 2011 Natural variation in life history and aging phenotypes is associated with mitochondrial DNA deletion frequency in *Caenorhabditis briggsae*. BMC Evol. Biol. 11: 11. https://doi.org/10.1186/1471-2148-11-11

Fox, E. J., K. S. Reid-Bayliss, M. J. Emond, and L. A. Loeb, 2014 Accuracy of next generation sequencing platforms. Next Gener. Seq. Appl. 1: 1000106.

Greene, E. A., C. A. Codomo, N. E. Taylor, J. G. Henikoff, B. J. Till *et al.*, 2003 Spectrum of chemically induced mutations from a large-scale reverse-genetic screen in *Arabidopsis*. Genetics 164: 731–740.

Hadjivasiliou, Z., N. Lane, R. M. Seymour, and A. Pomiankowski, 2013 Dynamics of mitochondrial inheritance in the evolution of binary mating types and two sexes. Proc. Biol. Sci. 280: 20131920. https://doi.org/10.1098/rspb.2013.1920

Harrison, J. S., and R. S. Burton, 2006 Tracing hybrid Incompatibilities to single amino acid substitutions. Mol. Biol. Evol. 23: 559–564. https://doi.org/10.1093/molbev/msj058

Havird, J. C., and D. B. Sloan, 2016 The roles of mutation, selection, and expression in determining relative rates of evolution in mitochondrial *vs.* nuclear genomes. Mol. Biol. Evol. 33: 3042–3053. https://doi.org/10.1093/molbev/msw185

Havird, J. C., M. D. Hall, and D. K. Dowling, 2015a The evolution of sex: a new hypothesis based on mitochondrial mutational erosion. Bioessays 37: 951–958. https://doi.org/10.1002/bies.201500057

Havird, J. C., N. S. Whitehill, C. D. Snow, and D. B. Sloan, 2015b Conservative and compensatory evolution in oxidative phosphorylation complexes of angiosperms with highly divergent rates of mitochondrial genome evolution. Evolution 69: 3069–3081. https://doi.org/10.1111/evo.12808

Hicks, K. A., D. R. Denver, and S. Estes, 2013 Natural variation in *Caenorhabditis briggsae* mitochondrial form and function suggests a novel model of organelle dynamics. Mitochondrion 13: 44–51. https://doi.org/10.1016/j.mito.2012.12.006

Hill, G. E., 2015 Mitonuclear ecology. Mol. Biol. Evol. 32: 1917–1927. https://doi.org/10.1093/molbev/msv104

Hu, Z-L., J. Bao, and M. Reecy, 2008 CateGOrizer: A web-based program to batch analyze gene ontology classification categories. Online J. Bioinform. 9: 108–112.

Joyner-Matos, J., L. C. Bean, H. L. Richardson, T. Sammeli, and C. F. Baer, 2011 No evidence of elevated germline mutation accumulation under oxidative stress in *Caenorhabditis elegans*. Genetics 189: 1439–1447. https://doi.org/10.1534/genetics.111.133660

Jun, A. S., I. A. Trounce, M. D. Brown, J. M. Shoffner, and D. C. Wallace, 1996 Use of transmitochondrial cybrids to assign a complex I defect to the mitochondrial DNA-encoded NADH dehydrogenase subunit 6 gene mutation at nucleotide pair 14459 that causes Leber hereditary optic neuropathy and dystonia. Mol. Cell. Biol. 16: 771–777. https://doi.org/10.1128/MCB.16.3.771

Kayser, E. B., P. G. Morgan, and M. M. Sedensky, 1999 GAS-1: a mitochondrial protein controls sensitivity to volatile anesthetics in the nematode *Caenorhabditis elegans*. Anesthesiology 90: 545–554. https://doi.org/10.1097/00000542-199902000-00031

Kayser, E. B., P. G. Morgan, C. L. Hoppel, and M. M. Sedensky, 2001 Mitochondrial expression and function of GAS-1 in *Caenorhabditis elegans*. J. Biol. Chem. 276: 20551–20558. https://doi.org/10.1074/jbc.M011066200

Kayser, E. B., M. M. Sedensky, and P. G. Morgan, 2004 The effects of complex I function and oxidative damage on lifespan and anesthetic sensitivity in *Caenorhabditis elegans*. Mech. Ageing Dev. 125: 455–464. https://doi.org/10.1016/j.mad.2004.04.002

Kim, Y., K. S. Schumaker, and J.-K. Zhu, 2006 EMS mutagenesis of *Arabidopsis*. Methods Mol. Biol. 323: 101–103.

Kimura, M., 1983 *The Neutral Theory of Molecular Evolution*. Cambridge University Press, Cambridge. https://doi.org/10.1017/CBO9780511623486

Kofler, R., and C. Schlotterer, 2012 Gowinda: unbiased analysis of gene set enrichment for genome-wide association studies. Bioinformatics 28: 2084–2085. https://doi.org/10.1093/bioinformatics/bts315

Konrad, A., O. Thompson, R. H. Waterston, D. G. Moerman, P. D. Keightley *et al.*, 2017 Mitochondrial mutation Rate, spectrum and heteroplasmy in *Caenorhabditis elegans* spontaneous mutation accumulation lines of differing population size. Mol. Biol. Evol. 34: msx051. https://doi.org/10.1093/molbev/msx051

Kowald, A., and T. B. Kirkwood, 2011 Evolution of the mitochondrial fusion-fission cycle and its role in aging. Proc. Natl. Acad. Sci. USA 108: 10237–10242 (erratum: Proc. Natl. Acad. Sci. USA 108: 16481). https://doi.org/10.1073/pnas.1101604108

Kurki, S., V. Zickermann, M. Kervinen, I. Hassinen, and M. Finel, 2000 Mutagenesis of three conserved Glu residues in a bacterial homologue of the ND1 subunit of complex I affects ubiquinone reduction kinetics but not inhibition by dicyclohexylcarbodiimide. Biochemistry 39: 13496–13502. https://doi.org/10.1021/bi001134s

Kuznetsov, A. V., and R. Margreiter, 2009 Heterogeneity of mitochondria and mitochondrial function within cells as another level of mitochondrial complexity. Int. J. Mol. Sci. 10: 1911–1929. https://doi.org/10.3390/ijms10041911

Lane, N., 2011 Mitonuclear match: optimizing fitness and fertility over generations drives ageing within generations. Bioessays 33: 860–869. https://doi.org/10.1002/bies.201100051

Lenaz, G., R. Fato, M. L. Genova, C. Bergamini, C. Bianchi *et al.*, 2006 Mitochondrial Complex I: structural and functional aspects. Biochim. Biophys. Acta 1757: 1406–1420. https://doi.org/10.1016/j.bbabio.2006.05.007

Lynch, M., 1996 Mutation accumulation in transfer RNAs: molecular evidence for Muller's ratchet in mitochondrial genomes. Mol. Biol. Evol. 13: 209–220. https://doi.org/10.1093/oxfordjournals.molbev.a025557

McDonald, M. J., D. P. Rice, and M. M. Desai, 2016 Sex speeds adaptation by altering the dynamics of molecular evolution. Nature 531: 233–236. https://doi.org/10.1038/nature17143

Meiklejohn, C. D., K. L. Montooth, and D. M. Rand, 2007 Positive and negative selection on the mitochondrial genome. Trends Genet. 23: 259–263. https://doi.org/10.1016/j.tig.2007.03.008

Montooth, K. L., C. D. Meiklejohn, D. N. Abt, and D. M. Rand, 2010 Mitochondrial-nuclear epistasis affects fitness within species but does not contribute to fixed incompatibilities between species of *Drosophila*. Evolution. 64: 3364–3379. https://doi.org/10.1111/j.1558-5646.2010.01077.x

Morran, L. T., M. D. Parmenter, and P. C. Phillips, 2009 Mutation load and rapid adaptation favour outcrossing over self-fertilization. Nature 462: 350–352. https://doi.org/10.1038/nature08496

Osada, N., and H. Akashi, 2012 Mitochondrial-nuclear interactions and accelerated compensatory evolution: evidence from the primate cytochrome c oxidase complex. Mol. Biol. Evol. 29: 337–346. https://doi.org/10.1093/molbev/msr211

Otto, S. P., and M. W. Feldman, 1997 Deleterious mutations, variable epistatic interactions, and the evolution of recombination. Theor. Popul. Biol. 51: 134–147. https://doi.org/10.1006/tpbi.1997.1301

Pätsi, J., M. Kervinen, M. Finel, and I. E. Hassinen, 2008 Leber hereditary optic neuropathy mutations in the ND6 subunit of mitochondrial complex I affect ubiquinone reduction kinetics in a bacterial model of the enzyme. Biochem. J. 409: 129–137. https://doi.org/10.1042/BJ20070866

Phillips, W. S., A. L. Coleman-Hulbert, E. S. Weiss, D. K. Howe, S. Ping *et al.*, 2015 Selfish mitochondrial DNA proliferates and diversifies in small, but not large, experimental populations of *Caenorhabditis briggsae*. Genome Biol. Evol. 7: 2023–2037. https://doi.org/10.1093/gbe/evv116

Radzvilavicius, A. L., 2016 Mitochondrial genome erosion and the evolution of sex. Bioessays 38: 941–942. https://doi.org/10.1002/bies.201600148

Radzvilavicius, A., H. Kokko, and J. Christie, 2017 Mitigating mitochondrial genome erosion without recombination. Genetics 207: 1079–1088. https://doi.org/10.1534/genetics.117.300273

Rand, D. M., 2001 The units of selection on mitochondrial DNA. Annu. Rev. Ecol. Syst. 32: 415–448. https://doi.org/10.1146/annurev.ecolsys.32.081501.114109

Rand, D. M., 2008 Mitigating mutational meltdown in mammalian mitochondria. PLoS Biol. 6: e35. https://doi.org/10.1371/journal.pbio.0060035

Rand, D. M., R. A. Haney, and A. J. Fry, 2004 Cytonuclear coevolution: the genomics of cooperation. Trends Ecol. Evol. 19: 645–653. https://doi.org/10.1016/j.tree.2004.10.003

Rawson, P. D., and R. S. Burton, 2002 Functional coadaptation between cytochrome c and cytochrome c oxidase within allopatric populations of a marine copepod. Proc. Natl. Acad. Sci. USA 99: 12955–12958. https://doi.org/10.1073/pnas.202335899

Sackton, T. B., R. A. Haney, and D. M. Rand, 2003 Cytonuclear coadaptation in *Drosophila*: disruption of cytochrome c oxidase activity in backcross genotypes. Evolution 57: 2315–2325. https://doi.org/10.1111/j.0014-3820.2003.tb00243.x

Sato-Carlton, A., X. Li, O. Crawley, S. Testori, E. Martinez-Perez *et al.*, 2014 Protein phosphatase 4 promotes chromosome pairing and synapsis, and contributes to maintaining crossover competence with increasing age. PLoS Genet. 10: e1004638. https://doi.org/10.1371/journal.pgen.1004638

Sazanov, L. A., 2015 A giant molecular proton pump: structure and mechanism of respiratory complex I. Nat. Rev. Mol. Cell Biol. 16: 375–388. https://doi.org/10.1038/nrm3997

Sharp, N. P., and S. P. Otto, 2016 Evolution of sex: using experimental genomics to select among competing theories. Bioessays 38: 751–757. https://doi.org/10.1002/bies.201600074

Shiraishi, Y., M. Murai, N. Sakiyama, K. Ifuku, and H. Miyoshi, 2012 Fenpyroximate binds to the interface between PSST and 49 kDa subunits in mitochondrial NADH-ubiquinone oxidoreductase. Biochemistry 51: 1953–1963. https://doi.org/10.1021/bi300047h

Shoubridge, E. A., 2001 Cytochrome c oxidase deficiency. Am. J. Med. Genet. 106: 46–52. https://doi.org/10.1002/ajmg.1378

Skipper, M., C. A. Milne, and J. Hodgkin, 1999 Genetic and molecular analysis of fox-1, a numerator element involved in Caenorhabditis elegans primary sex determination. Genetics 151: 617–631.

Smith, S. W., L. C. Latta, D. R. Denver, and S. Estes, 2014 Endogenous ROS levels in *C. elegans* under exogenous stress support revision of oxidative stress theory of life-history tradeoffs. BMC Evol. Biol. 14: 161. https://doi.org/10.1186/s12862-014-0161-8

Stewart, A. D., and P. C. Phillips, 2002 Selection and maintenance of androdioecy *in Caenorhabditis elegans*. Genetics 160: 975–982.

Sumiyoshi, E., A. Sugimoto, and M. Yamamoto, 2002 Protein phosphatase 4 is required for centrosome maturation in mitosis and sperm meiosis in *C. elegans*. J. Cell Sci. 115: 1403–1410.

Taylor, D. R., C. Zeyl, and E. Cooke, 2002 Conflicting levels of selection in the accumulation of mitochondrial defects in Saccharomyces cerevisiae. Proc. Natl. Acad. Sci. USA 99: 3690–3694. https://doi.org/10.1073/pnas.072660299

Teotonio, H., S. Carvalho, D. Manoel, M. Roque, and I. M. Chelo, 2012 Evolution of outcrossing in experimental populations of *Caenorhabditis elegans*. PLoS One 7: e35811. https://doi.org/10.1371/journal.pone.0035811

Twig, G., B. B. Hyde, and O. S. Shirihai, 2008 Mitochondrial fusion, fission and autophagy as a quality control axis: the bioenergetic view. Biochim. Biophys. Acta 1777: 1092–1097. https://doi.org/10.1016/j.bbabio.2008.05.001

Vassilieva, L. L., A. M. Hook, and M. Lynch, 2000 The fitness effects of spontaneous mutations in *Caenorhabditis elegans*. Evolution 54: 1234–1246. https://doi.org/10.1111/j.0014-3820.2000.tb00557.x

Vasta, V., M. Sedensky, P. Morgan, and S. H. Hahn, 2011 Altered redox status of coenzyme Q9 reflects mitochondrial electron transport chain deficiencies in *Caenorhabditis elegans*. Mitochondrion 11: 136–138. https://doi.org/10.1016/j.mito.2010.09.002

Wernick, R. I., S. Estes, D. K. Howe, and D. R. Denver, 2016 Paths of heritable mitochondrial DNA mutation and heteroplasmy in reference and *gas-1* strains of *Caenorhabditis elegans*. Front. Genet. 7: 1–12. https://doi.org/10.3389/fgene.2016.00051

Whitlock, A. O. B., K. M. Peck, R. B. R. Azevedo, and C. L. Burch, 2016 An evolving genetic architecture interacts with Hill-Robertson interference to determine the benefit of sex. Genetics 203: 923–936. https://doi.org/10.1534/genetics.116.186916

Zeeberg, B. R., W. Feng, G. Wang, M. D. Wang, A. T. Fojo *et al.*, 2003 GoMiner: a resource for biological interpretation of genomic and proteomic data. Genome Biol. 4: R28. https://doi.org/10.1186/gb-2003-4-4-r28

Communicating editor: A. Agrawal